Research Trends in Air Pollution Control: Scrubbing, Hot Gas Clean-up, Sampling and Analysis

R. Mahalingam, and
Alfred J. Engel, editors

Research Trends in Air Pollution Control: Scrubbing, Hot Gas Clean-up, Sampling and Analysis

R. Mahalingham, and Alfred J. Engel, editors

Theodore G. Brna
Stuart W. Churchill
Paul T. Cunningham
A. S. Damle
David L. Etherton
Dale A. Furlong
T. L. Holmes
Stanley A. Johnson
John J. Kalvinskas
Samir P. Kothari
Romesh Kumar
Noam Lior
R. Mahalingham
Chat P. Mohan
Ronald L. Ostop
Avinash N. Patkar
D. T. Pratt
Alan D. Randolph
Naresh Rohatgi
Eric A. Samuel
J. Thomas Schrodt
S.-K. Tang
B. K. Thota

AIChE Symposium Series

Number 211 1981 Volume 77

Published by

American Institute of Chemical Engineers

345 East 47 Street New York, N. Y. 10017

American Institute of Chemical Engineers
345 East 47 Street, New York, N.Y. 10017

Library of Congress Cataloging in Publication Data
Main entry under title:

Research trends in air pollution control. :

(AIChE symposium series ; no. 211)
1. Flue gases—Purification—Addresses, essays, lectures. I. Mahlingam, R., 1938- . II. Engel, Alfred J. III. Series.
TD885.R47 628.5'32 81-19133
ISSN 0065-8812 AACR2
ISBN 0-8169-0219-4

Printed in the United States of America by
Lew A. Cummings Co., Inc.

FOREWORD

Chemical engineers and other professionals have a key role to play in the preservation of the environment, in addition to economic and efficient operation of process plants. Additionally, they have the responsibility of recycling the key components from the effluent streams, wherever feasible, in order to conserve our valuable resources.

The theme of the AIChE 89th National Meeting held in Portland, Oregon, in August 1980 was "Use of Renewable and Non-Renewable Resources—A Challenge for the Future". Five symposia in the Air area were held at this meeting to reflect the above theme. The sessions were Air Pollution Transport, Hot Gas Clean-Up (2 sessions), Air Pollution Sampling and Analysis, and Recent Trends in Control Practices for Industrial Emissions. At the 73rd Annual AIChE Meeting in Chicago in November 1980, no specific sessions dealing with air pollution were held, but four sessions on coal research and coal use were presented. Between these two AIChE meetings, a total of 59 papers were presented. Some of these have already appeared in *Chemical Engineering Progress* and some others are scheduled to appear in the AIChE Symposium Series on coal. Out of the remaining papers, those printed here represent a wide diversity of interest and should be of lasting value. No doubt there were other equally qualified papers presented that could not be included here because of space limitations.

The editors hope that the papers in this volume will be a resource material for a long time and will be useful in opening up investigations along new avenues.

In addition to the various session chairmen and co-chairmen who deserve our thanks, one person who deserves special thanks here is Charles A. Brown, a graduate student at Washington State University and presently a graduate student at the University of Washington.

R. Mahalingam, *editor*
Washington State University
Pullman, Washington

A. J. Engel, *editor*
Pennsylvania State University
University Park, Pennsylvania

CONTENTS

FUEL GAS DESULFURIZATION IN FLUIDIZED-BEDS OF GASIFIER WASTE ASHES

J. THOMAS SCHRODT

Department of Chemical Engineering
University of Kentucky
Lexington, Kentucky 40506

CHAT P. MOHAN

Monsanto Chemical Company
St. Louis, Missouri

Gasifier ashes, inherently containing iron oxides, show excellent high temperature reactivity for the H_2S, COS, and CS_2 found in low energy coal gases. Data gathered from small fluid beds of four selected ashes contacted with synthesized gases containing H_2S support the good performance and efficiency of his desulfurization process. Solid phase diffusion of ionic iron in the particles, carbon deposition, ash regeneration, and secondary process reactions are discussed.

A significant fraction of the sulfur in coal appears in the pyrite (FeS_2) and sulfate ($FeSO_4$) forms. During coal gasification the iron is oxidized to hematite (Fe_2O_3) and magnetite (Fe_3O_4) and rejected as part of the bottoms ash. The sulfur is converted to hydrogen sulfide (H_2S) and lesser amounts of carbon disulfide (CS_2) and carbonyl sulfide (COS). Although these sulfur compounds account for less than one mole percent of the product fuel gas, they must be removed before combustion for environmental reasons and to prevent corrosion to process and combustion equipment. If desulfurization is carried out while the fuel gas is still at gasifier exit conditions, i.e. 800° to 1200°K and 1 to 100 atmospheres pressure, 5 to 10 percent of the heating value of the fuel can be retained in the form of sensible heat. These facts provide incentive for development of new high temperature desulfurization processes. Murthy, et al. (1977), Edwards (1979), Morrison (1979), Schrodt and Hahn (1976), and Mohan (1980) have reviewed the most recent developments in this field of hot gas cleanup.

Our objective in this work is to determine if gasifier bottoms ashes containing iron oxides can effectively remove hydrogen sulfide from hot, made-up fuel gases, when the latter are passed through small fluidized-beds of the ashes. We seek to identify through X-Ray and Energy Dispersive Analyses of the solids, and influent and effluent gas analyses, the gas, and gas-solid reactions, and the effects of several selected parameters on these. Through careful reduction of the effluent gas concentration data we seek to identify the rate controlling reaction steps, and to develop and verify global, fluid-bed models.

EXPERIMENTAL

Three gasifier ashes, containing 5 to 23 weight percent Fe_2O_3 were selected for testing as the solid reactants. These were crushed and three U.S.-Mesh sized fractions: 70/80, 80/120, and 120/170, were prepared. The chemical, physical, and fine particle characteristics of these are reported in the dissertation of the junior author (Mohan, 1980).

The desulfurization tests were carried out at atmospheric pressure in a 20-mm x 100-mm quartz tube with a porous, quartz disc fused to the inner wall. This disc supported the ash, which was fluidized to about 2X the minimum fluidization velocity by a synthesized fuel gas of nominal composition: 20% CO, 10% H_2, 17% CO_2, 3% CH_4, 49% N_2, and the remainder H_2S (0.5 to 1.0%). Gas compositions were measured by a dual column GC equipped with a TC detector and an on-line CDS. The gases were preheated before contacting the ash bed. The quartz tube was located in a ±1.0°K controlled high-temperature furnace and

0065-8812-81-4308-0211-$2.00.

temperatures were monitored via quartz-sheathed chromel-alumel thermocouples.

Before and during the reaction studies, the fluidizing and decrepitation behavior of the ashes was observed both at room temperature, and at 756°, 811°, 922°, and 1033°K. No significant decrepitation of any of the four ashes in the three sized fractions was measured after 10 days of fluidization at room temperature nor after 60 days at the higher temperatures. At 1033°K ash particles tended to adhere to one another and to the wall of the tube. Continuous, uniform fluidization at this high temperature was judged difficult. At 2X the minimum fluidization velocity, the bed showed an expansion of about 1.8, with good solid mixing.

RESULTS AND DISCUSSION

Desulfurization started at the entrance of the sorbent bed and progressed under a concentration wave of H2S that moved very slowly within a reaction zone through the bed. In front of the reaction zone, where $H_2/H_2S >> 100$ and $CO/CO_2 \cong 1.6$, Fe_2O_3 in the ash was rapidly reduced to Fe_3O_4 and sometimes even to $Fe_{.95}O$ (wüstite):

$$3Fe_2O_3 + H_2 \rightarrow 2Fe_3O_4 + H_2O \qquad K_{1000°K} = 1.0 \times 10^5 \qquad (1)$$

$$3Fe_2O_3 + CO \rightarrow 2Fe_3O_4 + CO_2 \qquad K_{1000°K} = 1.1 \times 10^5 \qquad (2)$$

$$Fe_3O_4 + H_2 \rightarrow 3FeO + H_2O \qquad K_{1000°K} = 0.34 \qquad (3)$$

$$Fe_3O_4 + CO \rightarrow 3FeO + CO_2 \qquad K_{1000°K} = 0.63 \qquad (4)$$

Powder X-Ray scans on fresh, and pretreated ash recovered from the reactor after a brief exposure to the reducing gases are shown in Figure 1. The diffraction patterns of these two scans strongly support the occurrance of reactions (1) and (2). Sharp increases and decreases in the initial concentrations of CO_2 and H_2O; and CO and H_2 respectively were also noted, and support the reduction reactions. The Fe-O-S phase diagram presented in Figure 2 indicates a thermodynamic correctness to the above conclusions.

It was also noted that CO, CO_2, H_2, and H_2O reached near equilibrium concentrations relative to the water-gas-shift reaction:

$$CO + H_2O \rightarrow CO + H_2 \qquad K_{1000°K} = 1.75 \qquad (5)$$

Product to reactant concentration ratios for this reaction were 2.7 and 2.0 at 922° and 1033°K, while the corresponding theoretical values of K are 2.2 and 1.5, respectively. At lower temperatures, reaction rates were so low that apparently equilibrium could not be attained. Evans (1975) measured reaction rates for the reverse water-gas-shift reaction, homogeneously, and over reduced, and sulfided ashes and concluded the reaction is catalyzed by minerals in the ash. Surprisingly, sulfidation of the magnetite did not affect the reaction rate.

As the fuel gas entered the fluidized-bed, reaction commenced between H2S and Fe_3O_4 and/or $Fe_{.95}O$:

$$Fe_3O_4 + 3H_2S + H_2 \rightarrow 3FeS + 4H_2O \qquad K_{1000°K} = 2.67 \times 10^7 \qquad (6)$$

$$FeO + H_2S \rightarrow FeS + H_2O \qquad K_{1000°K} = 4.21 \times 10^2 \qquad (7)$$

Large equilibrium constants favor complete removal of the sulfides from the gas. The solid sulfide is actually pyrrhotite, $Fe_{.9470}$. X-Ray analyses shown in Figure 1 of fully sulfided ashes indicate pyrrhotite is the only iron sulfide formed during desulfurization. This finding is contrary to results reported by Schultz and Berber (1970) but in agreement with those of Joshi and Leuenberger (1977). According to the phase diagram shown in Figure 2, this is the only stable solid sulfide that could reside in the bed at the prevailing conditions. At temperatures below 1000°K the H_2/H_2S ratio has to be less than 6.5×10^{-3} to have pyrite as the stable sulfide; this concentration ratio is unlikely to occur during

fuel gas processing. For long on-stream times there was no detectable gaseous sulfide in the effluents. The concentration wave of H_2S was formed near the inlet and moved through the bed at a rate dependent upon the availability of unreacted iron and hydrogen sulfide.

As the availability of reactant iron oxide in the bed diminished, measurable and increasing concentrations of two sulfide gases: carbonyl sulfide (COS) and H_2S broke through the bed. In Figure 3, which shows this result, it should be noted that the sum of the steady-state exit concentrations of COS and H_2S equals the inlet concentration of H_2S. The presence of the COS is a result of dehydrogenation of H_2S according to the equation:

$$H_2S + CO_2 \rightarrow COS + H_2O \quad K_{1000°K} = 0.033 \quad (8)$$

At all temperatures investigated reaction (8) was found to be at equilibrium. An identical result was also reported by Schrodt (1978) in some earlier fixed-bed studies on this system.

When fully sulfided ashes were fluidized with streams of 3 percent O_2 in N_2, the sulfur in the pyrrhotite was released as SO_2:

$$2FeS + 7/2\ O_2 \rightarrow Fe_2O_3 + 2SO_2 \qquad K_{1000°K} = 10^{90} \quad (9)$$

Unlike the earlier fixed-bed studies, no significant amount of elemental sulfur was formed.

Total ash sulfur capacities are evaluated by the equation:

$$M_o = \frac{QC_{AO}}{q} \int_o^{t_E} \left(1 - \frac{C_A}{C_{AO}}\right) dt \quad (10)$$

where t_E = time when $C_A/C_{AO} \rightarrow 1.0$, and sorption bed efficiencies by the equation:

$$\tau_{0.1} = \frac{QC_{AO}t_{0.1}}{M_o q} \quad (11)$$

where here $t_{0.1}$ = time when $C_A/C_{AO} \rightarrow 0.1$. Tau is a dimensionless time. M_o and $\tau_{0.1}$ were parameters used to evaluate the effects of the independent variables on the desulfurization reaction rates. These effects were examined from plots of C_A/C_{AO} versus τ.

M_o was expected to be a function of the inherent iron in the ashes only; however, it was discovered that fresh ashes - those which had not been subjected to a series of sorption-regeneration cycles - had sulfur capacities that were only a fraction of their theoretical capacity. As the number of cyclic uses was increased, as illustrated in Figure 4, the values of M_o and $\tau_{0.1}$ also increased and reached constant values after 6 to 10 cycles. With a Western Kentucky No. 9 ash containing 22.13 weight percent Fe_2O_3, a stabilized value of $M_o = 1.17 \times 10^{-3}$ g mol/g ash and $\tau_{0.1} = 0.835$ was reached at 922°K. When the desulfurization temperature was suddenly decreased from 922° to 810°K, the values of Mo and $\tau_{0.1}$ also decreased, as shown in Figure 4, and stabilized at lower values.

Analyses of random particles of ash by SEM and EDAX show that the cyclic phenomenon is related to a diffusion of iron from within the core of the particles to the surface structure of the pores as indicated in Figure 5. Figure 6 shows the reproducibility of the fluidized-bed data after stabilization of the ash.

Additional data show that ash capacity and efficiency increase with temperature (Figure 7), Fe_2O_3 concentration, and decreasing fluid velocity. Some selected results are presented in Table 1.

MATHEMATICAL MODEL

The reaction of H_2S with Fe_3O_4 within ash particles involves the following transport and kinetic steps:

- Diffusion of H_2S from the bulk gas phase to the solid particle.
- Diffusion of H_2S through interstices of the particle to reaction sites.
- Chemical reaction of H_2S with unreacted Fe_3O_4.
- Counter-diffusion of the product gas, H_2O, out of the solid.

SEM analyses showed the oxide is concentrated after cyclic use in a thin layer near the particle surface. The layers approximate flat plates of thickness 10 to 50 μ fixed by the parent iron oxide concentrations. Two asymptotic regimes of reaction control are suggested: a region of chemical control where Fe_3O_4 grains react in a spatially uniform way with a uniform concentration of H_2S, and a region of diffusion control where reactant gas diffuses through interstices and reacts

rapidly at a sharp solid product-reactant interface.

Unlike the previously cited fixed-bed desulfurization studies in which the concentration breakthrough curves were mirror images of the inner bed, reaction concentrations, the breakthrough curves from the fluidized-bed studies were more logically images of the final stages of reaction of all the solid particles in the bed. Therefore, when the effluent concentration data were applied to global reaction rate models, the parameters deduced are at best representative of the final stages of reaction.

A uniform chemical reaction rate model describes the sulfide breakthrough data test. When material balances were developed for the sulfur components in both the gas the solid phases with the basic assumptions of (1) isothermal plug-flow, (2) first order gas kinetics, (3) irreversible reaction, (4) pseudo steady-state relative to bed and particles, (5) perfect solid mixing, and (6) uniform dispersal of H_2S in the solid, the following coupled dimensionless equations were obtained:

$$\frac{d\bar{Y}}{d\bar{Z}} = \frac{\bar{Y}\bar{X}^m}{N_K + N_F\bar{X}^m} \tag{12}$$

$$\frac{d\bar{X}}{d\tau} = 1 - \exp\left[\frac{-\bar{X}^m}{N_K + N_F\bar{X}^m}\right] \tag{13}$$

where

$$N_K \equiv \frac{u}{Lk_v W_o^m \rho_B} \tag{14}$$

$$N_F \equiv \frac{uR}{3Lk_m(1-\varepsilon)}$$

$$\bar{Y} \equiv \frac{C_A}{C_{AO}},\quad \bar{X} \equiv \frac{W}{W_o},\quad \bar{Z} \equiv \frac{1}{L} \tag{15}$$

To estimate the mass transfer parameter K_F, a value for the mass transfer coefficient k_m was necessary. The following correlation from Kunii and Levenspiel (1969) was selected:

$$\frac{k_m d_p}{D_m} = 0.374\ Re^{1.18} \tag{16}$$

For all test runs $Re \cong 1.0$, $k_m \cong 1.0$ cm/sec and $K_m \cong 0.01$ to 0.02.

Equations (12) and (13) were coded for Fourth Order Runge-Kutta solution. The parameters to be determined were m, the exponent on the solid reactant concentration, and N_K, the reaction rate parameter. Through trial and error procedure, curves generated for m = 2 were found to best match the breakthrough curves of 38 test runs. A similar procedure was used to arrive at values of N_K and from these the kinetic rate constants, k_v was calculated. These were statistically analyzed to check for the effects of the operating variables. The temperature effect was expressed by the Arrhenius relationship and the following correlation was obtained:

$$k_v = k_o\, C_{AO}^{'a} \left(\frac{u}{u_{mf}}\right)^b e^{-E/RT} \tag{17}$$

Values of the parameters are listed here:

$$k_o = 2.49 \times 10^{13}\ \frac{\text{g ash-cm}^3}{(\text{gmol } Fe_2O_3)^2\ \text{min}}$$

$$E = 10{,}882\ \text{cal/gmol}$$

$$a = -1.48$$

$$b = -0.788$$

The proper rate expression is

$$-R_A = k_v C_A W^2 \tag{18}$$

Figure 8 shows a predicted sulfide breakthrough curve and the declining concentration of Fe_2O_3 within the fluidized-bed reactor for one run with actual data superimposed.

It is believed that this work will help to support the development of a continuous process for desulfurizing hot coal-derived fuel gases.

ACKNOWLEDGEMENT

This work was supported by the U.S. Department of Energy under contract E-(40-1)-5076 and the Commonwealth of Kentucky through the Institute for Mining and Minerals Research.

NOMENCLATURE

C_A	Bulk concentration of gas reactant, gmol/cm^3
C_A'	Bulk concentration of gas reactant, mole %
D_m	Diffusivity of gas reactant in fuel, cm^2/sec
d_p	Mean particle diameter, cm
E	Activation energy, cal/gmol
K	Thermodynamic equilibrium constant
k_m	Mass transfer coefficient, cm/sec
k_v	Reaction rate constant, g ash-cm^3/(g mol Fe_2O_3)^2 min
L	Length of fluidized bed, cm
l	Position in bed, cm
M	Ash sorbate capacity, g mol/g ash
N_F	Parameter defined by Eq. (15)
N_K	Parameter defined by Eq. (14)
Q	Total flow rate of gas, cm^3/min
q	Ash load in bed, g
R	Gas law constant, cal/g mol °K
R_A	Reaction rate
Re	Reynolds number, $d_p u\rho/\mu$
T	Temperature, °K
t	Time, min
u	Fluid velocity, cm/min
W	Solid reactant concentration, g mol/g ash
$\overline{X}$	Dimensionless solid concentration
$\overline{Y}$	Dimensionless gas concentration
$\overline{Z}$	Dimensionless position in bed

GREEK LETTERS

ε	Porosity of bed
ρ_B	Bulk density of bed, g/cm^3
τ	Dimensionless time
$\tau_{0.1}$	Sorption efficiency

SUBSCRIPT

o	Initial value

LITERATURE CITED

M. S. Edwards, "H_2S-Removal Processes for Low-BTU Gas", Oak Ridge National Laboratory Report TM-6077, January 1979.

J. F. Evans, "Secondary Factors in the Hot Ash Desulfurization Process", M.S. Thesis, University of Kentucky, 1978.

D. K. Joshi and E. L. Leuenberger, "Hot Low BTU Producer Gas Desulfurization in Fixed Bed of Iron Oxide-Hy Ash", U.S. Department of Energy Report Fe-2033-19, September 1977.

D. Kunii and O. Levenspiel, "Fluidization Engineering", p. 200, John Wiley & Son, New York, 1969.

C. P. Mohan, "Desulfurization of Fuel Gases in Fluidized Beds of Gasifier Waste Ashes", Ph.D. Dissertation, University of Kentucky, December 1980.

G. F. Morrison, "Hot Gas Cleanup", IEA Coal Research Report ICTIS/TR 03, March 1979.

B. N. Murthy, et al., "Fuel Gas Cleanup Technology for Coal Gasification", U.S. Department of Energy Report FE-2220-15, March 1977.

J. T. Schrodt and O. J. Hahn, "Hot Fuel Gas Desulfurization", Report IMMR 15-PDII-76, University of Kentucky, May 1976.

J. T. Schrodt, "Hot Gas Desulfurization with Gasifier Ash Sorbents", Proceedings of the Symposium on Potential Health and Environmental Effects of Synthetic Fossil Fuel Technologies, 32, July 1979.

F. G. Schultz and J. S. Berber, "Hydrogen Sulfide Removal from Hot Producer Gas with Sintered Absorbents", Jour. of Air Pollution Control Assoc., 20, 93, 1970.

TABLE 1. Selected Desulfurization Results

Run	Ash	Fe_2O_3 (wt%)	Particle Size cm	Temperature °K	Fluid Velocity cm/sec	Sulfur Capacity of Ash g/100g	$T_{0.1}$
061	W.Ky. 9	22.13	0.0151	1033	8.11	3.98	0.865
049	W.Ky. 9	22.13	0.0151	922	7.26	3.74	0.833
053	W.Ky. 9	22.13	0.0151	811	6.52	3.17	0.705
058	W.Ky. 9	22.13	0.0151	756	6.07	3.19	0.663
075	W.Ky. 9	22.13	0.0107	811	5.58	4.12	0.726
126	W.Ky. 9	22.13	0.0151	811	9.55	4.21	0.700
095	Elkhorn 3	9.51	0.01935	811	6.80	1.29	0.550
111	Rosebud	8.19	0.01935	811	6.80	1.07	0.630

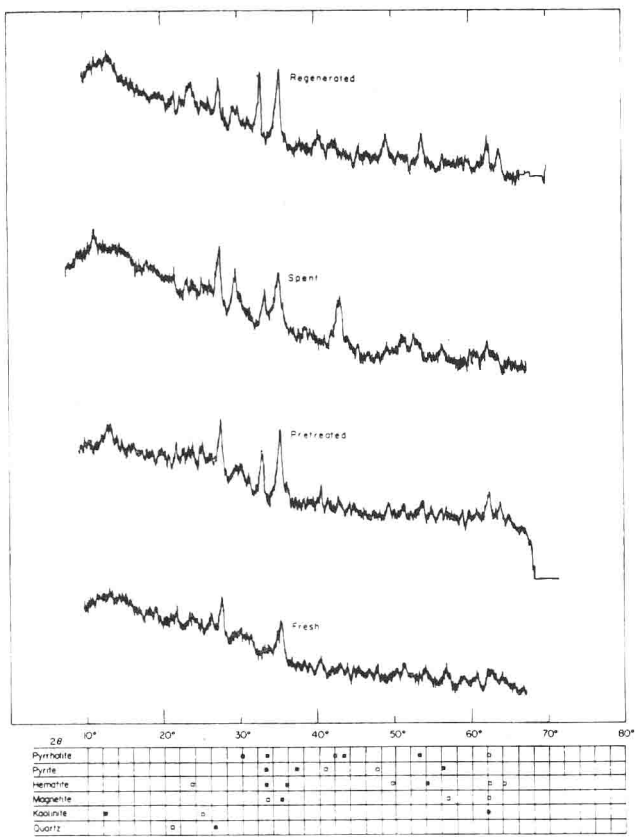

Figure 1. X-ray analyses of fresh, pretreated, spent and regenerated Western Ky. No. 9 coal ash. (■ primary and □ secondary peaks)

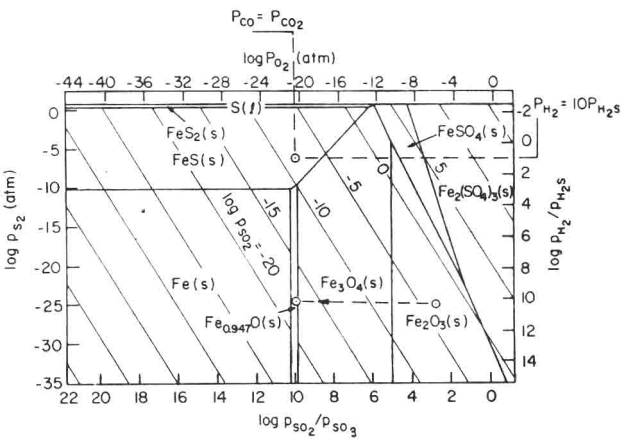

Figure 2. Thermochemistry of iron-sulfur-oxygen at 1000°K.

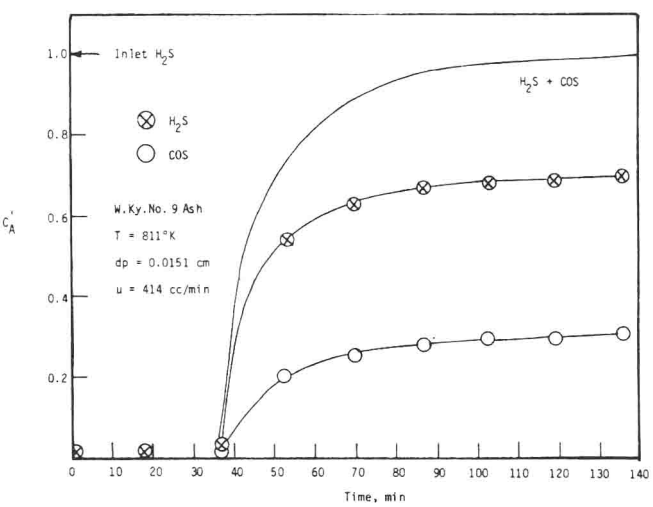

Figure 3. Breakthrough curves for COS, H_2S, and COS + H_2S.

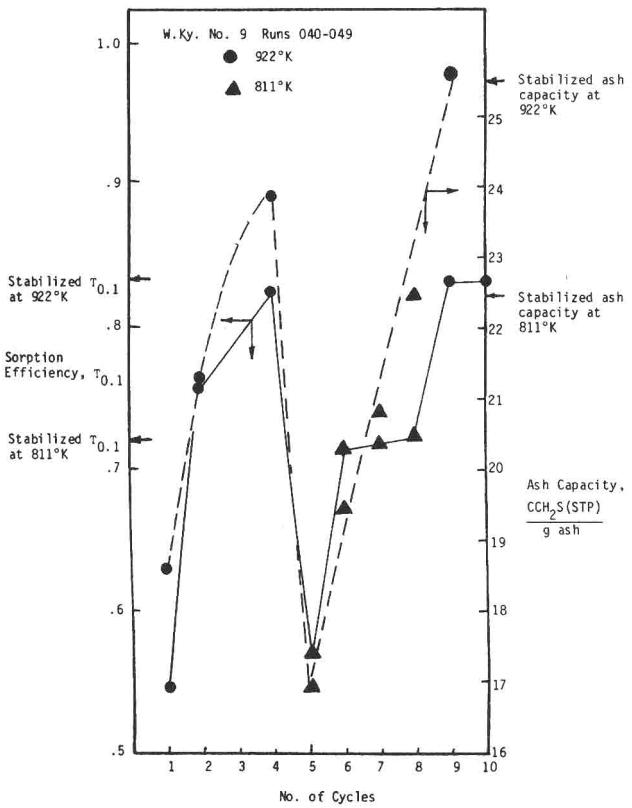

Figure 4. Ash sulfur capacities and sorption efficiencies as a function of cyclic use.

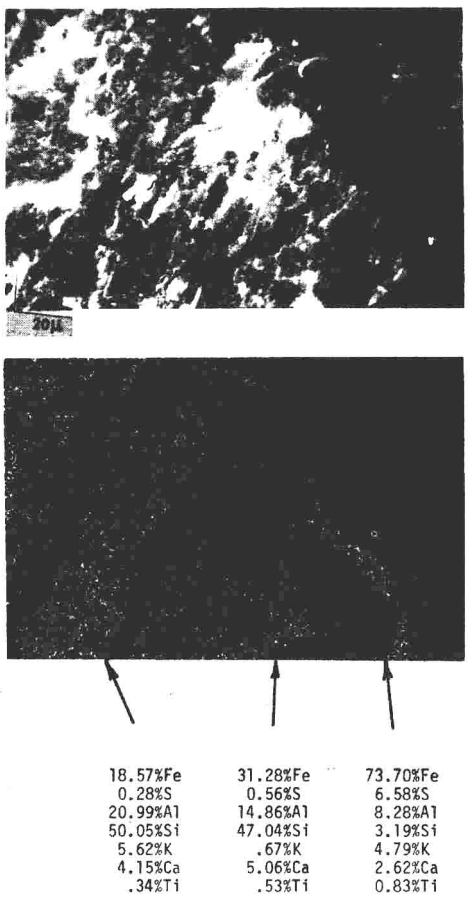

18.57%Fe	31.28%Fe	73.70%Fe
0.28%S	0.56%S	6.58%S
20.99%Al	14.86%Al	8.28%Al
50.05%Si	47.04%Si	3.19%Si
5.62%K	.67%K	4.79%K
4.15%Ca	5.06%Ca	2.62%Ca
.34%Ti	.53%Ti	0.83%Ti

Figure 5. Scanning electron micrograph of cross section of ash particle after ten regenerations with air. Right hand picture shows qualitative distribution of iron. EDAX results indicate high iron concentrations along edge of particle with residual sulfur.

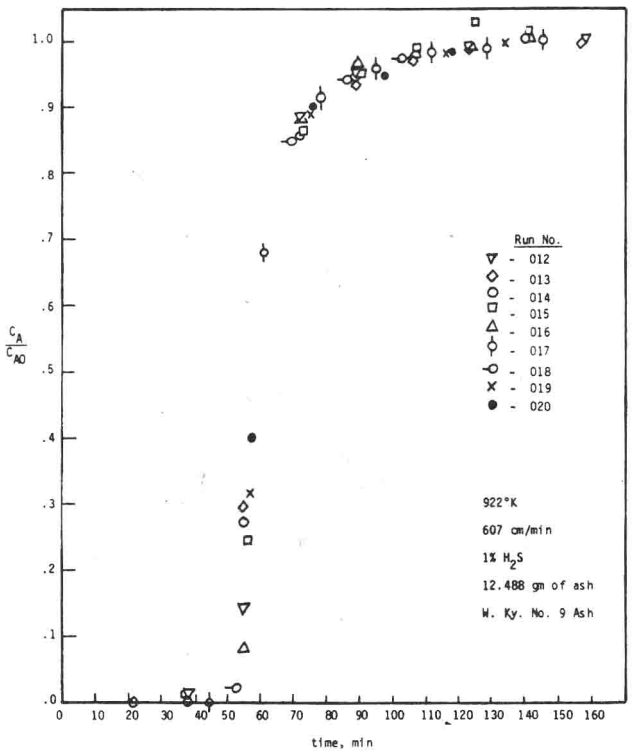

Figure 6. Reproducibility of desulfurization rate data.

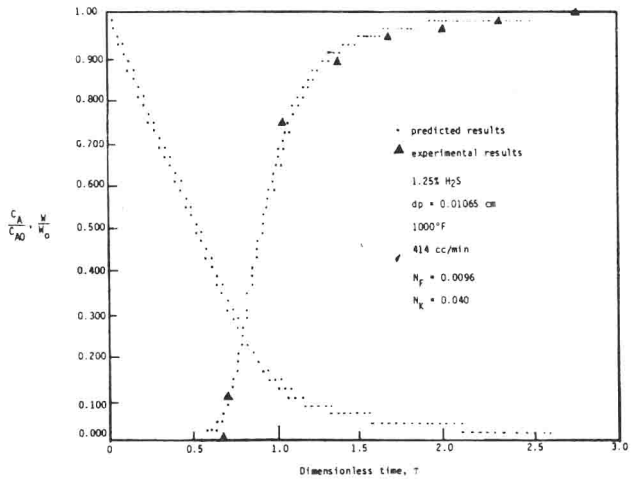

Figure 8. Dimensionless breakthrough curves: predicted by mathematical model and actual data.

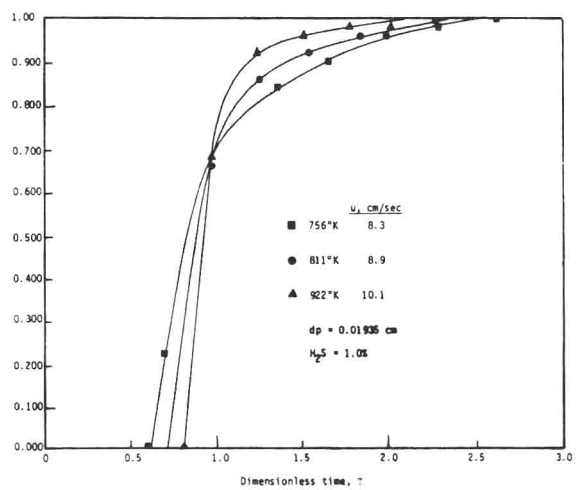

Figure 7. Presentation of rate data in dimensionless form to show effect of temperature.

CATALYSTS DEVELOPMENT AND EVALUATION IN THE CONTROL OF HIGH-TEMPERATURE NO_x EMISSIONS

Supported catalysts, which could effectively reduce NO_x emissions from high temperature sources, were developed and evaluated. The variables studied were the inlet concentration of NO_x, the gas hourly space velocity, and the effect of the presence of a reducing agent.

Experimental work involved the passing of gas mixtures containing NO_x through a heated catalyst bed 10 cm long and contained inside a 2.7 cm I.D. ceramic tube. In selecting the catalyst, particular attention was paid to its stability under the given operating conditions (about 1000°C and slightly above atmospheric pressures) for possible placement in the immediate vicinity of the combustion zone. Supported nickel and supported cobalt oxide catalysts have been studied. Reaction section inlet and exit gas streams were analyzed for NO_x concentrations with a chemiluminescent NO/NO_x analyzer.

Results from this work show that the supported nickel catalyst is relatively more effective for NO_x decomposition. When, however, carbon monoxide in excess was introduced into the reaction gases, chemical reduction approaching 100 percent NO_x removal on both supported nickel and supported cobalt catalysts was observed.

R. MAHALIGAM
B. K. THOTA
and
D. T. PRATT

Department of Chemical Engineering
Washington State University
Pullman, Washington, 99164

Oxides of nitrogen have been identified as toxic air pollutants and efforts are being directed towards alleviating the problem by controlling their emissions. Out of a total NO_X emission of 20 million tons per year, combustion of fuel is by far the largest stationary and mobile source of NO_X (1). 55% of all NO_X emissions originate from stationary combustion sources, 40% from mobile sources, and the rest from chemical process industries, etc. The combustion sources are boilers, internal combustion engines, gas turbines, and incinerators. Gas turbines in electric utilities (2) and in heavy-duty vehicular applications are expected to grow at phenomenal rates. New Source Performance Standards (NSPS) for NO_X are expected to be tightened in future years, especially with increase in concern over secondary particulate formation and acid rain (3).

Extensive research has been and is currently being carried out to cope with the problem of NO_X emission from different sources. Very few publications, if any, have come out dealing with NO_X emission problems arising from high temperature sources. Conventional methods applicable to automobile exhaust emission control may not work or may need modifications for situations where high temperatures and large volumes of exhaust gases occur.

BACKGROUND

Formation of NO_X

NO_X refers to the sum of nitric oxide (NO) and NO_2. Oxides evolved from the nitrogen present in the fuel are called fuel NO_X while those that evolve from the nitrogen in the combustion air are termed thermal NO_X.

Nitric oxide formation in combustion processes proceeds according to the following reactions:

$$N_2 + O \rightleftarrows NO + N \quad (1)$$

$$N + O_2 \rightleftarrows NO + O \quad (2)$$

Reactions 1 and 2 contribute approximately equal amounts of NO (4). Given time, these reactions continue to an equilibrium level, which is influenced by variables such as flame temperature, residence time, concentration of each gas, and movement of the gases through zones of different temperatures, pressures, and concentrations. Once NO is formed, the rate of decomposition is slow under ordinary reaction conditions. As a result, NO concentration is frozen in the com-

---

B. K. Thota is now at DuPont, Charleston, WV.
D. T. Pratt is at University of Michigan, Ann Arbor, MI 48109.

0065-8812-81-4180-0211-$2.00

bustion products after they leave the high temperature zone. The NO thus formed can further react with oxygen to form NO_2 as follows:

$$NO + 1/2\ O_2 \rightleftarrows NO_2 \qquad (3)$$

The above reaction demonstrates the coexistence of NO and NO_2. The stability of NO_2 decreases with increasing temperature (5). Consequently, only a small percentage of the total nitrogen oxide emissions is NO_2.

The rate of NO formation from N_2 and O_2 is very highly temperature-dependent. Zeldovich (6) gives the following expression for the rate of formation of NO, derived on the basis of the chain mechanism:

$$\frac{d\,[NO]}{dt} = 3.0 \times 10^{14} e^{-129{,}000/RT} [N_2][O_2]^{1/2}$$

where: [NO], $[N_2]$, $[O_2]$ = concentrations, gram mole/cm^3; t = time, seconds; T = temperature, degrees Kelvin; R = gas constant, cal/gram mole-°K.

The high activation energy for NO formation accounts for the extreme dependence of reaction rate on temperature. The gas-phase decomposition has a lower, but still appreciable activation energy.

NO_x formation also varies according to the type of combustion involved. In a homogeneous combustion process, fuel and air are intimately and uniformly mixed before combustion. In the case of the heterogeneous combustion process typical of the diesel and gas turbine engines, in which fuel and air mix and burn simultaneously, the chemical reactions resulting in NO formation are unchanged but the physical environment in which these reactions proceed is quite different from that of the homogeneous system (7).

The theoretical prediction of NO (or NO_x) production in a gas turbine combustor is an exceedingly difficult problem since the reaction rate and, hence, the total NO_x formed depends on the time-temperature history of the reactants (8). The time-temperature history is difficult to determine since the fluid dynamics of the combustor reaction zone is complex and not well understood. For engineering purposes, a simple correlation is often used to predict the effect of various operating variables on NO_x emissions. This correlation is of the form:

$$NO_x = A\ P_4^{a} T_3^{b} \exp(T_3/c)\ f^{d}$$

where A, a, b, c, d are constants, P_4 is the combustor pressure, T_3 is the combustor air inlet temperature and f is the overall combustor fuel-to-air mass ratio. An additional multiplier needed is τ, the residence time.

Decomposition of NO

The reactions influencing nitric oxide decomposition are the bimolecular atom exchange reactions between nitric oxide and nitrogen atoms, between nitric oxide and nitrogen atoms, between nitric oxide and oxygen atoms (the reverse of the NO formation reactions), and between pairs of NO molecules.

$$NO + N \rightarrow N_2 + O \qquad (4)$$

$$NO + O \rightarrow N + O_2 \qquad (5)$$

$$NO + NO \rightarrow N_2O + O \qquad (6)$$

NO decomposition by Reactions 4 and 5 is about 500 times more than that by Reaction 6. Reaction 5 is endothermic and therefore much less favorable energetically than Reaction 4. The large number of oxygen atoms relative to nitrogen atoms present in the system tends to compensate for this, however, and the Reactions 4 and 5 proceed at about the same forward rate (7).

As in all chemical reactions, the rates of formation and decomposition for NO can be hastened by means of catalysts; while catalysts cannot change equilibrium concentrations, they reduce the time of attainment of equilibrium. A number of investigators have studied the NO decomposition reaction and they have come out with different results (9, 10, 11). Some (9, 12) have indicated that NO decomposition is heterogeneous below 1000°K. They also suggest Reactions 4, 5, and 6 as the only possible reactions, although it is not agreed as to which reaction is predominant. It also appears that there is some variation and uncertainty in the kinetic parameters presented by various investigators (13).

Control Techniques for NO_x Emissions

Some of the methods used for reducing NO_x emissions include limiting fuel nitrogen content, low excess air firing, staged combustion, "off-stoichiometric firing," flue gas recirculation, water and steam injection, selective or nonselective catalytic reduction as well as combinations of these techniques 3, 14 to 19, 46).

Catalytic Treatment of NO_x

Catalytic treatment of exhaust gases to control NO_x emissions is a viable and possible technique. Two major treatment processes are catalytic decomposition of NO and catalytic reduction of NO.

Decomposition of NO to its elements appears to be thermodynamically favorable in the temperature range of 300 to 4000° K (13). The decomposition reaction is

$$2\ NO \rightarrow N_2 + O_2 \qquad (7)$$

Catalytic reduction of NO is achieved by mixing a reducing agent such as CH_4, H_2, or CO into the gas and passing the mixture over a catalyst in a chamber. Some of the possible chemical reactions are

$$2NO + 2CO \rightarrow N_2 + 2CO_2 \qquad (8)$$

$$2NO + 2H_2 \rightarrow N_2 + 2H_2O \qquad (9)$$

The reaction chamber effluent contains mostly N_2, CO_2, and H_2O.

More than 600 NO_x catalysts on various supports have been developed and evaluated on automotive exhaust systems. Compounds of 36 individual metals or combinations and several alloys have been used to make catalysts on about 20 different supports. In tests involving automotive exhaust gases at space velocities in the range of 15,000 to 50,000 Hr^{-1}, none was found to be effective for NO decomposition (46). Many of the above catalysts, however, proved to be excellent promoters for the reduction of NO_x by CO, H_2, or hydrocarbons (HC) present in exhaust gases. The life of a catalyst is limited by the temperature to which it is exposed, the oxidizing tendency of the flue gas, attrition losses during operation, and presence of poisons.

In addition to observing catalytic NO removal when a CO-NO-N_2 mixture was reacted, Taylor (20) also found extensive NO removal (up to 77%) from NO-N_2 mixtures at a temperature of 215° C without any added reducing agent. The catalyst employed was alumina-supported barium-promoted copper chromite. Sakaida, et al. (21), using a platinum-nickel-alumina catalyst determined that NO decomposition was second order at 425° to 540°C and 1 to 15 atmospheres. Sourirajan and Blumenthal (22) studied NO_x reduction by CO and H_2 between 100° to 550° C at compositions of 300 to 1500 ppm and reported CuO-silica to be the best catalyst. Roth and Doerr (23) continued on the work of Taylor using supported CuO, CuO-Cr_2O_3 catalysts. Baker and Doerr (4) reported the formation of NH_3 in the presence of water vapor. Ayen and Peters (24) investigated NO reduction with hydrogen. In their work, Jones et al. (25), showed that some selectivity toward NO reduction by H_2 on noble metals is obtained at stoichiometric engine operations. Bauerle, et al. (26), studied the reduction of NO by CO in the presence of O_2 at 320°C using several copper-based and noble metal catalysts.

In another study using infrared spectroscopy, London and Bell (27) studied the reduction of NO by CO on silica supported copper oxide and postulated that nitric oxide can dissociate upon adsorption. Amirnazmi, et al. (28), studied the aspect of oxygen inhibition on the rate of NO decomposition on metal oxides and platinum between 450° and 1000°C, around atmospheric pressure. They found that the reaction was first order with respect to NO and that above 450°C, N_2 and O_2 were the only products. Wise and French (29) reported NO decomposition to be second order in the range of 600° to 1000°C, the reaction being surface-catalyzed below 730°C and homogeneous at higher temperatures. Yuan, et al. (12), have shown NO removal to be heterogeneous in a zero-order reaction below 1100°C, and homogeneous in a second order reaction above 1400°C. Between 1100°C and 1400°C, both heterogeneous and homogeneous reactions took place simultaneously, the contribution from each depending on the area of the surface, and its chemical nature, as well as on the temperature and concentration. In their study of flash desorption of nitric oxide from tungsten, Yates and Madey (30) found that at high temperatures, NO was dissociated on the surface with an activation energy of 46.7 K-cal $mole^{-1}$.

Klimisch and Taylor (31) noticed dual functionality and synergistic effects with catalysts containing nickel in combination with copper, platinum, or palladium. Among these catalysts the ammonia decomposition function resides primarily in the nickel while the reduction activity is obtained from the other metal. Bartholomew (32) reported that monolithic-supported Pd-Ni and Pd-Ru catalysts are effective in NO_x removal; but he indicated that longterm stability of these catalysts is a serious problem. CO and C_3H_6, along with the NO_x, were used in the gas streams and the temperature range in

these investigations was 480°C to 600°C. Recently, General Motors Research Laboratories (33) have come up with a report on catalytic NO reduction studies and mentioned that ruthenium selectively catalyzes NO conversion reaction, practically without any ammonia formation. This work was performed in a reducing atmosphere using both hydrogen and carbon monoxide. The maximum temperature employed in this case was around 600°C. Several catalysts have been offered for NO_x control depending on NO_x sources, concentrations, conditions, etc., and most of these are covered by patents (34). In Table 1 is given a summary of catalytic NO studies by various authors.

In spite of these investigations, there seem to be wide areas of disagreement between the published results presented by different authors. In addition, not much significant work has been done in the area of catalytic studies relevant to NO_x control from turbine emissions, which typically occur at temperatures around 1000°C and higher and roughly at atmospheric pressure.

EQUIPMENT AND PROCEDURE

Flow Equipment

In the flow arrangement shown in Figure 1, gases first entered the mixing chamber, then the preheater. From the preheater, the gas mixture was directed into the reactor. The equipment was designed such that continuous analysis of the inlet and exit gas streams for NO_x was possible.

The mixing chamber was a 30 cm long, 3.4 cm I.D., and 0.64 cm thick lucite tube. A ceramic tube, 2.54 cm I.D. and 54 cm long, containing 0.64 cm Intalox-saddle packing served as the gas preheater. The preheater tube was placed in a horizontal fashion in a Lindberg Hevi-Duty Type 167 electric furnace, which was capable of heating up to 1000°C.

The reactor section consisted of a 2.7 cm I.D., 76 cm long Leco ceramic tube with one end tapered (Figure 2). The actual catalytic reactor was a 10 cm cylindrical cage of diameter very close to the i.d. of the reactor tube and made of #16 stainless steel screen (16 mesh). The cage was supported on a tube made up of a threaded portion 14 cm long 0.95 cm O.D. stainless steel tube, and a 30 cm long 0.64 cm O.D. stainless steel tube, joined together by plasma welding. The end of the support tube near the catalyst cage was sealed. The cage was held in position onto the support tube by means of stainless steel nuts. In subsequent runs, a slight modification of this arrangement was made. The catalyst cage was replaced by just two end screens to hold the catalyst in place. A chromel-alumel thermocouple insulated by a series of 5.0 cm long double-hole ceramic insulators, was embedded in the catalyst bed. The thermocouple wires with insulators were run through the support tube. The chromel-alumel thermocouple was stipulated by the manufacturer (Hoskins Mfg. Co.) to be accurate to within ±3/4 percent in the temperature range of 280 to 1269°C. The open end of the support tube was sealed using Sauereisen electro temp cement No. 8, after the thermocouple was connected to a D.C. millivoltmeter.

The inlet sample was collected using a 0.32 cm O.D. stainless steel sample probe installed just at the upstream (inlet) end of the catalyst bed. The inlet sample probe, the support tube, and a 0.48 cm O.D. stainless steel tube, used as exhaust outlet, all were incorporated in the stainless steel seal assembly.

The tapered end of the reactor tube was connected to the gas line from preheater, by means of a Cajon ultra-torr adaptor and Swagelok connections. The sealing of this end was ensured using Sauereisen cement.

The reactor tube was heated by means of a Lindberg CF-1 combustion tube laboratory furnace. The voltage on the heating elements could be varied by means of built-in transformers. A heating length of about 20 cm was obtainable in this furnace. The reactor tube was horizontally suspended in the furnace so that it was coaxial with the heating section of the furnace. This arrangement enabled the reactor tube and hence the catalyst bed to be exposed to uniform heating.

The exhaust line from the reactor was led into a hood vent by means of a 0.48 cm O.D. stainless steel tube. This exhaust line was branched off at the reactor unit and led to the analyzing equipment for monitoring exit gases. The pressure of the gas stream entering the reactor tube was measured by a pressure gauge. A platinum-platinum +13% rhodium thermocouple measured the temperature of the reactor tube.

Gas Analyses

The inlet and the exit sample lines from the reactor tube were led through the Thermoelectron Model 44 Chemiluminescent NO-NO_x analyzer. Since the NO_x analyzer measured